JOURNAL OF APPLIED ELECTROCHEMISTRY **28** (1998) 971–977

Effects of current density on adhesion of copper electrodeposits to polyimide substrates

G. A. PRENTICE

Department of Chemical Engineering, University of Detroit Mercy, Detroit, MI 48219, USA

K. S. CHEN

Engineering Sciences Center, Sandia National Laboratories, Albuquerque, NM 87185-0826, USA

Received 21 April 1997; revised 19 January 1998

To provide protection, electrical conductivity, or a decorative finish, plastic components are often metallized by a three-step process: deposition of a catalytic palladium layer followed by electroless and electrolytic plating. In this paper we focused on determining the relationship between applied current density used to electrodeposit copper and adhesion of the metal to a polyimide substrate. To test a range of current densities on a single sample, we deposited a series of copper strips on a planar sheet of the polyimide material and electrodeposited copper in a modified Hull cell. From peel tests we found that strips subjected to higher current density adhered more strongly to the substrate. This experimental procedure should be generally applicable to other metal-polymer systems.

Keywords: *plating*, *plastic*, *copper*, *polyimide*, *current density*, *adhesion*

1. Introduction

The deposition of metal on plastic is routinely used in the fabrication of decorative parts in the automotive industry. Other applications include protective coatings, electromagnetic shielding, and conductors for electric current in microelectronic applications [1, 2]. Polymeric substrates are often metallized by palladium catalysis followed by electroless and electrolytic plating to provide surface protection and to add functionality. There is also interest in employing similar techniques in the fabrication of microelectronic devices. Polymer substrates provide a flexible, lightweight, insulated support for plated conductors and interconnects in microelectronic applications [3].

Catalytic palladium has traditionally been produced on a substrate surface by immersion in a $PdCl_2/SnCl_2$ solution with subsequent chemical reduction of Pd^{2+} to Pd metal [4, 5]. An alternative method is to deposit onto the substrate a layer of catalyst solution, which is composed of palladium salt (e.g., palladium chloride) dispersed in a polymer-carrier dissolved in a solvent. The solvent is removed by hot-air drying, and the catalytic palladium clusters are generated by thermal activation (e.g., Tokas *et al.* [6]). We employed this thermal activation method in our present study to catalyse the substrate surface for depositing the seed metal layer via electroless plating of copper.

In all engineering applications, proper adhesion of the plated metal to the substrate is critical in maintaining appearance, device integrity or electrical continuity. A number of studies have been undertaken to determine the effects of materials and deposition processes on the strength of the metal-polymer bond. Surface modification of the polymeric substrate is usually effective in promoting adhesion. Baumgartner [7] and Baumgartner and Scott [8] showed that adhesion could be improved through mechanical or chemical surface modification, and they reported that moisture at the metal-polymer interface adversely affects adhesion. Krause and Speckhard [9] found that adhesion could drop by an order of magnitude if significant moisture was present at the interface. To maximize the production rate of plated parts, it is advantageous to operate at high current densities; however, the effect of local current density on adhesion has not previously been analyzed quantitatively.

To study the effects of current density on adhesion, we prepared samples from planar sheets of polyimide material and deposited a series of strips from palladium-based material. In preparation for the electrolytic plating process, these strips were covered with a thin layer of copper through electroless plating. This planar sample was fixed in the plating bath at 45° to a planar counterelectrode with the result that each vertical copper strip was maintained at a current density that was approximately uniform.

In this modified Hull cell configuration, we were able to maintain a range of current densities on the strips with high current densities on the strips closer to the counterelectrode and lower current densities on strips farther removed from the counterelectrode. From peel tests conducted on individual strips, we were able to determine the effect of current density on adhesive strength.

0021-891X

2. Experimental details

Polarization data were obtained from a rotating disk electrode. By rotating the disk at several different rates, we determined the effects of hydrodynamics. In the experiments performed in a plating bath, solution stirring was provided by bubbling air through the electrolyte solution. We observed that the air stirring was vigorous, and from approximate calculations we determined that it would be sufficient to prevent significant concentration gradients at the electrode surface.

We used a Pine Instruments model ASR rotator and a PAR model 273 potentiostat to control the electrode potential. Electrodes of 0.3 cm^2 area were rotated at speeds ranging from $0 - 300$ rpm. Linear potential scans were begun at 0.0 V with respect to a copper reference electrode. The sweep rate was 10 mV s^{-1} and covered a range between -1.2 and 0.8 V corresponding to current densities between -1000 to 500 mA cm^{-2}. The magnitude of the maximum experimental current densities were less than 100 mA cm^{-2}; therefore, the range of our polarization experiments was sufficient to cover the entire range of interest.

Initially, we used samples of the copper material plated on the polyimide; however, because this was thin material plated on a polymeric substrate, it was difficult to adapt to our standard disk holder. We ran several experiments with both the plated material and pure copper for comparison. We found little difference in polarization curves; therefore, for convenience we ran a series of experiments with 99.9% pure copper. Experiments were run at room temperature (28 °C) to correspond to plating conditions.

The plating bath was the actual solution that had been used and maintained over the past year. The original solution was specified to have a composition of 7.6 g dm^{-3} Cu, 190 g dm^{-3} sulfuric acid, and 60 ppm chloride. The commercial product is Lea-Ronal Acid Copper Plating Solution 20019. A brightener, Copper Gleam PC, was added to the original solution at a concentration of 0.5% by volume.

Over the current density range of interest, we observed little difference between the cathodic and anodic scans when the electrodes were rotated at 300 rpm. This result indicated that the electrode surface was not significantly altered by sweeps in either direction and that concentration gradients were sufficiently small to avoid producing significant concentration overpotential.

As expected, the electrodes with no stirring showed greater polarization at higher current densities. Because of copper ion depletion near the electrode surface, concentration overpotential altered the shape of the current density curve at cathodic potentials on the reverse sweep. Curves generated with stagnant solution were used to understand the effects of concentration gradients but were not used to develop the polarization curves used in the simulations.

Data from the 300 rpm experiments were analysed and fit to a Butler-Volmer form using a Levenberg-Marquardt routine. The equation describing the current density i against overpotential η for our system is

$$i = 0.07\,[\exp(3.53\,\eta) - \exp(-2.54\,\eta)] \qquad (1)$$

The data and the curve described by this equation are shown in Fig. 1. This empirical polarization expression was used in all of the simulations of plating processes.

The cell used in the experiments consisted of a 36 cm cathode at a 45° angle to the anode. This arrangement is similar to a Hull cell; however, in the standard Hull cell, the cathode contacts the insulating walls that are perpendicular to the planar anode. We used an existing plating tank where the insulating walls were perpendicular to the anode but were not in contact with the cathode. In our cell the perpendicular insulated wall was about 16 cm from the left side of the cathode (the side nearest the counterelectrode),

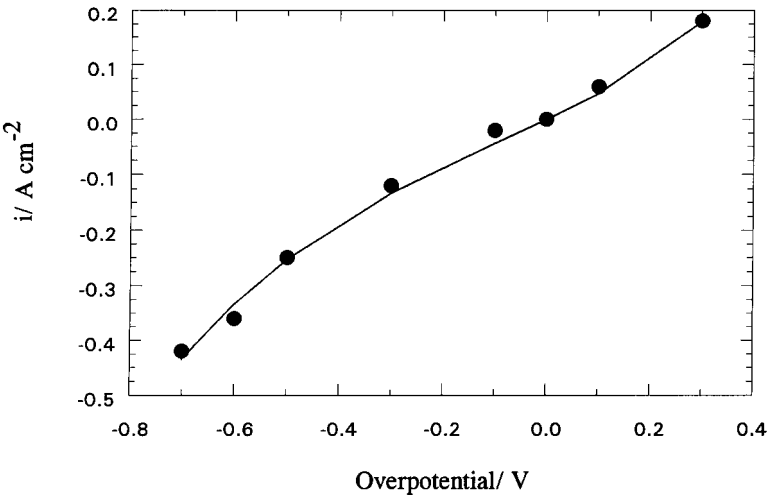

Fig. 1. Current density against overpotential for the copper electrode at 28 °C. Polarization data from a rotating disc electrode at 300 rpm (●). Solid line is a curve fitted to a Butler–Volmer expression ($i = 0.07[\exp(3.53\,\eta) - \exp(-2.54\,\eta)]$.

and the other insulated wall was 4 cm from the right side. This modification has the effect of increasing the current density near the edges of the cathode compared to the standard Hull cell; we refer to our experimental cell arrangement as a 'modified Hull cell'.

Minimum anode-cathode separation was 10 cm. The cathode consisted of a polymer backing on which seed-layer metallized strips had been deposited. The strips were 0.4 cm wide and separated by 0.32 cm. The anode was a series of bagged spheres along the 47 cm width of the tank. Solution agitation was provided by vigorous air stirring through a perforated tube along the bottom of the cathode.

Experiments were carried out at room temperature at a constant current of 5.5 A. The total area of the strips was 510 cm^2, and the average current density was approximately 0.01 A cm^{-2}. Under these conditions the applied voltage remained at 0.9 V with only small deviations from this value throughout the two-hour run. After each run the thickness of each strip on the cathode was measured and plotted.

3. Simulation of the current distribution on the cathode

In plating processes the metal distribution is proportional to the local current density. A model of the plating process can be developed from basic transport and thermodynamic principles [10]. The general strategy is to calculate the potential distribution from Laplace's equation. From the potential distribution the local current density is proportional to the local potential gradient, which is calculated at selected points along the electrode surface. At the electrolyte-electrode interface, overpotentials arise primarily due to kinetic resistance. For our system the current density and overpotential were determined by an iterative solution from an initial estimate of the potential distribution.

4. Governing equations

When the electrolytic medium can be considered to be homogeneous, the potential distribution is governed by Laplace's equation [11]

$$\nabla^2\phi = 0 \tag{2}$$

where ϕ is the potential in solution. The current density is calculated from the gradient of the potential

$$i = -\kappa\nabla\phi \tag{3}$$

where i is the current density and κ is the electrolyte conductivity. Overpotential η is defined as a departure from the equilibrium electrode potential. When measured with a reference electrode of the same type as the electrode material, the overpotential is defined by

$$\eta = V - \phi_0 \tag{4}$$

where ϕ_0 is the potential immediately adjacent to the electrode. The overpotential is related to the magnitude of the current density through a polarization expression such as Equation 1.

$$\eta = f(i) \tag{5}$$

5. Numerical methods

The simulations were performed using a finite difference technique. To simplify the description of the geometry, curved surfaces were approximated by a series of straight lines. A grid composed of square subdomains is imposed on the area representing the two-dimensional projection of the electrolyte solution. This area is completely bounded by surfaces representing electrodes or insulated surfaces.

Initial estimates of the potentials were automatically generated at each of the mesh points. In a plating cell all of the potentials in the electrolyte solution must fall between the potentials imposed on the anodes and cathodes. This principle was used in making initial estimates.

In the outer loop of the routine, iteration proceeds until a loose convergence of the potentials is reached. Numerical differentiation of the potential is performed at each electrode mesh point. In the inner loop, the local current density is calculated from the potential gradient and the electrolyte conductivity. Local values of the overpotential are obtained from the experimentally-determined polarization expressions.

In a converged solution, the value of the overpotential calculated from the Butler-Volmer equation must agree with that obtained from the definition of overpotential as a departure from the electrode potential $\eta = V - \phi_0$. If agreement is not obtained (within the specified tolerance), the value of ϕ_0 is adjusted through a programmed weighting algorithm. The new values of ϕ_0 are then used to define the boundary potentials used in Laplace's equation, and control is transferred back to the outer loop.

Upon convergence, the values of the local current density and the potential at each surface node (representing an electrode surface) are computed and sent to a file. The current density is numerically integrated over the surface area for each electrode to give values for the total current on all anodic surfaces and on all cathodic surfaces. Based on conservation of charge, the total cathodic current should be equal to the total anodic current. Deviations from equality give a measure of degree of convergence and of the degree of approximation in using the nearest node method (and the prescribed mesh size) to describe the geometric arrangement.

The degree of polarization can be characterized by the dimensionless Wagner number, Wa:

$$Wa = \frac{\kappa\left(\frac{\partial\eta}{\partial i}\right)}{L} \tag{6}$$

where the partial derivative is evaluated at the average current density and L is a characteristic length. For the Hull cell, L can be defined as the minimum anode-cathode separation subtracted from the maximum anode-cathode separation. The partial derivative characterizes charge-transfer resistance and the inverse of the conductivity characterizes an ohmic resistance in solution. If the Wagner number is on the order of one, then the kinetic component is substantial, and a primary current distribution cannot accurately describe the system. If the Wagner number is small, then ohmic resistance dominates, and the use of the primary current distribution model is justified.

In the modified Hull cell simulations presented in this investigation, we used a node spacing of 4 mm; for the entire domain approximately 12 000 mesh points were used. Our convergence criterion was a relative change in the average cathode potentials of 10^{-5} between iterations. Several minutes of computer time on a Pentium-based machine were required. Use of the nearest-node approximation caused some local variations in simulated current density, especially for low values of the Wagner number. Comparisons with the experimental and simulated results of Matlosz *et al.* [12] showed that our smoothed current density values were within a few percent of their results.

6. Comparison of experimental results with simulations

Experiments were carried out at room temperature in the modified Hull cell at a constant current of 5.5 A. Several assumptions were made in running the simulations. We modelled the cathode as a single continuous metallic plate. Because the potential varied by no more than 20 mV during each two-hour experiment, we assumed a constant applied potential in the simulation.

A plot of the simulated current density distribution appears in Fig. 2. Because the cathode does not contact the insulating walls, more current is able to concentrate at the two ends of the cathode; this phenomenon is known as the edge effect. The edge effect is observable in Fig. 2 in the range of 325–360 mm along the cathode. The cathodic current distribution has been calculated in a standard Hull cell over a range of Wagner numbers as defined in Equation 6 [12]. In a standard Hull cell where the cathode intersects the insulators, the current density monotonically decreases with distance from the anode.

As mentioned above, we did not use a standard Hull cell and, consequently, we could not use the results from Matlosz *et al.* [12]. If the cell dimensions used by Matlosz *et al.* were adopted for experiments, their theoretical results could be used directly. An experimental determination of the polarization curve would still be necessary to calculate the partial derivative in the Wagner number evaluation. In our cell the Wagner number was on the order of 0.01, which implies that we are operating in a region controlled by ohmic, rather than kinetic, effects.

Four experimental cathodes were run and the metal thicknesses measured. A typical plot appears in Fig. 3. All four samples display the same general characteristics. As expected, the metal is thickest near the edge closest to the anode. In all cases the minimum metal thickness occurs near, but not at, the edge farthest from the anode. The minimum metal thickness falls in a range from 20% to 35% of the maxi-

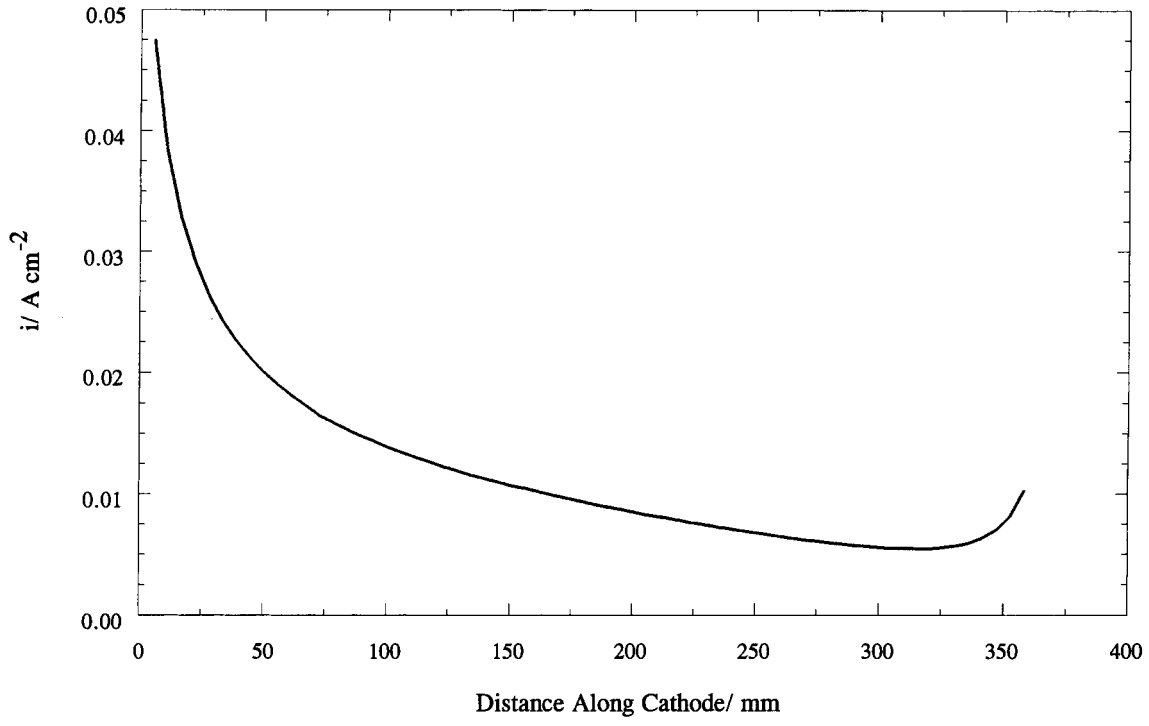

Fig. 2. Simulated current distribution of the modified Hull cell. Highest current density occurs nearest the counterelectrode.

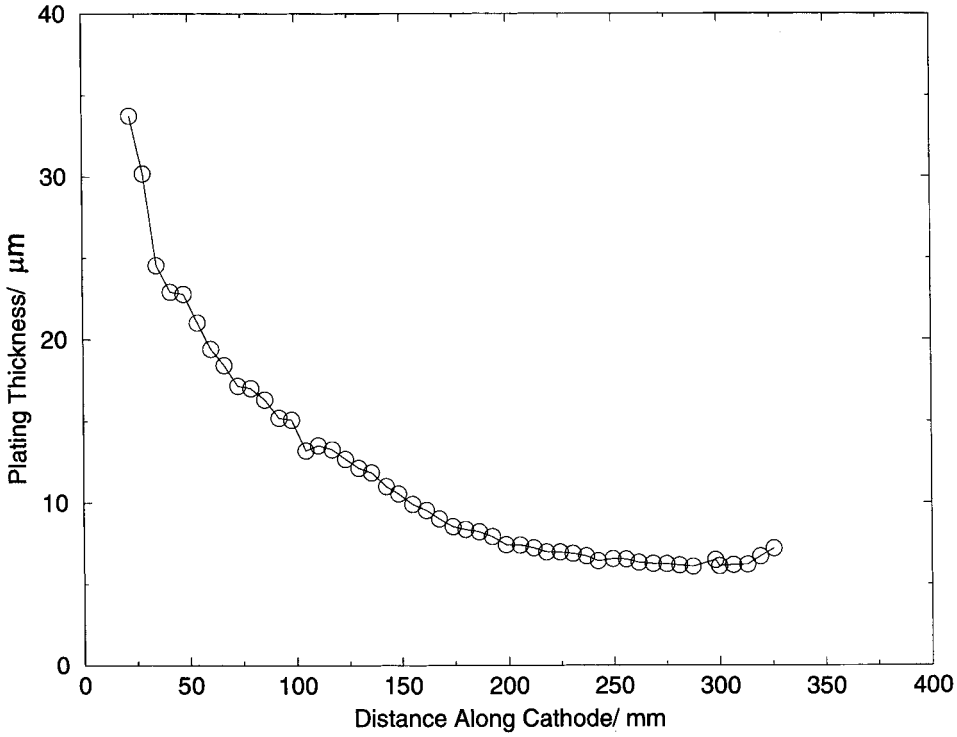

Fig. 3. Metal distribution on the cathode of the modified Hull cell.

mum thickness. This is somewhat more uniform than the predictions from the simulations, which show that the minimum current density is about 10% of the maximum current density.

The discrepancy between simulations and experiments may be attributed to several factors. Our simulations were based on short term polarization behaviour, which may change as the deposition process proceeds. From Faraday's law we calculated an overall current efficiency of about 60%; this may be partially due to actual inefficiency, and it may be partially due to small errors in thickness measurement, which result in errors in the calculated deposit mass. Our error analysis indicates that the primary measurement error results from variation in the thickness of a particular sample. These variations are on the order of 10% of the sample thickness or about 1 μm for the thinner samples and about 2 μm for the thicker samples. Faraday's law was also the basis for estimating local current densities from the experimental thickness measurements.

7. Adhesion results

The adhesion of the plated strips was measured by a 90° peel test using the IPC-TM-650 technique. The results plotted in Fig. 4 show that the adhesion is highest near the left side of the cathode. Because the left side of the cathode is nearest the counterelectrode, the current density is also highest in this region; therefore, this plot shows that the adhesive strength increases with current density. In the high current density area the adhesion is approximately 6 lb in^{-1}. In the lowest current density region the minimum peel strength is less than 1 lb in^{-1}, which is unacceptable in most applications.

Figure 5 shows that peel strength increases with deposit thickness. The increased metal thickness corresponds to the regions of higher current density. Again, this plot shows that adhesion is highest in regions of highest current density. Because all factors other than current density were the same, the difference in adhesion strength can be attributed to the differences in current density. Adhesive strength data reported in Figs 4 and 5 are from measurements in which the sample peeled at the bond. We did not include measurements in which either the metal strip or the substrate were torn.

We can only speculate on the possible causes of the correlation between adhesion and current density. One possibility is that the additional heating generated by the increased current promotes further curing of the metal-polymer bond. Heating of samples following plating has been reported to significantly influence adhesion. Previous experiments [8] showed that heating for 2 h at temperatures near 200 °C increased adhesion by a factor of four over room temperature samples. Adhesion dropped off rapidly at higher temperatures.

We can estimate the temperature increase in our samples from an energy balance. At steady-state, the heat generated from ohmic resistance in the thin metal strips is transferred to the solution through convective processes. This energy balance leads to the following equation for temperature rise ΔT (°C) as a function of current in a strip I (A), strip thickness x (cm), metal conductivity k (Ω^{-1} cm^{-1}), and convective heat transfer coefficient h (W cm^{-2} K^{-1})

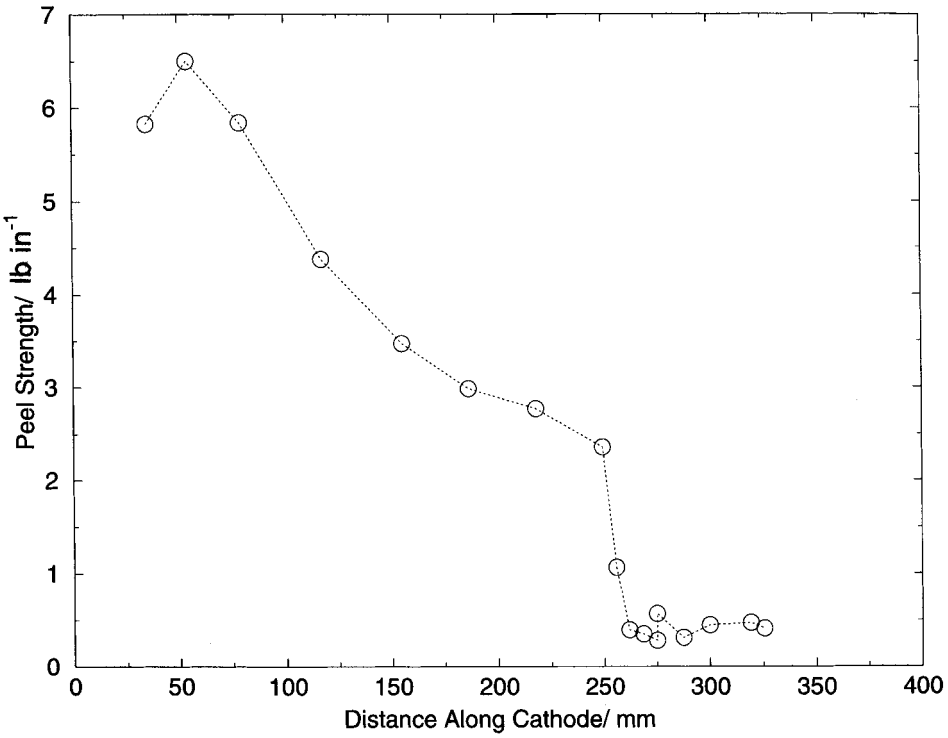

Fig. 4. Peel strength against distance along the cathode. The current density is highest at the left side of the cathode.

$$\Delta T = \frac{6.25 I^2}{hkx} \tag{7}$$

We assumed a heat transfer coefficient for forced convection caused by sparging of 6×10^{-3} W cm^{-2} K^{-1}. The conductivity for copper is $5 \times 10^5\ \Omega^{-1}$ cm^{-1}.

This analysis shows that the temperature difference increases as the square of the current and inversely with deposit thickness. The temperature difference is greatest at the beginning of the plating process when x is minimum. Also, current from the areas away from the current collector adds to the current from all the areas nearer the current collector; therefore, the maximum current in the strip occurs nearest the current collector. Consequently, the temperature within the deposit is also greatest at a point near the current collector. Putting all of these factors

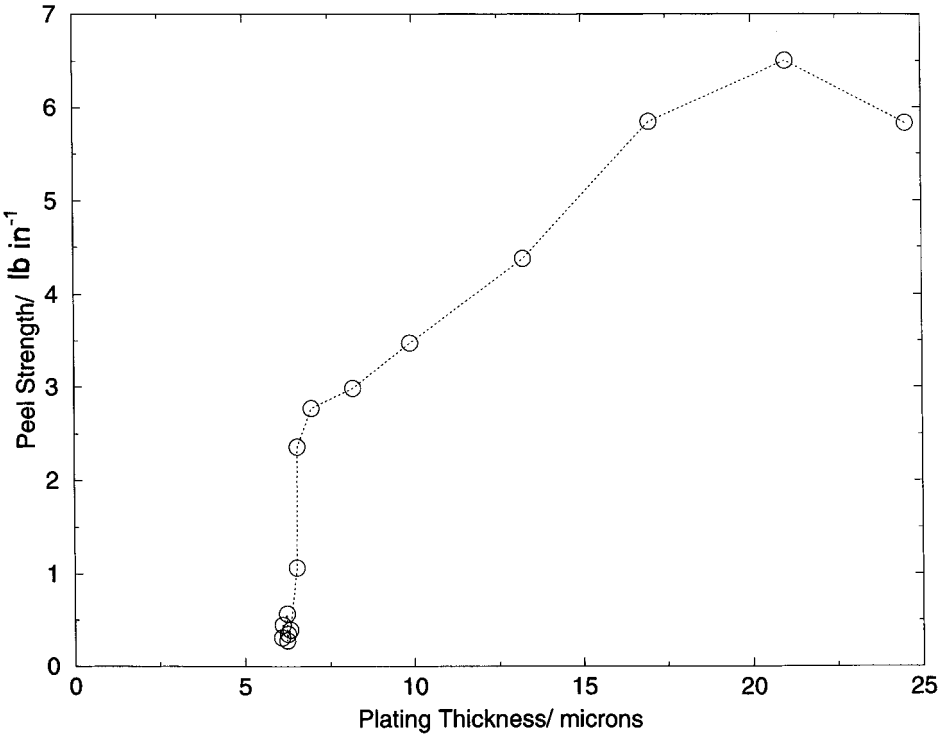

Fig. 5. Peel strength against plating thickness. Thicker deposits are also regions of higher current density.

together, the temperature in the deposit is greatest in the strip nearest the anode and in the section nearest the current collector at the beginning of the deposition process.

The thinnest deposit is near the beginning when $x \approx 10^{-5}$ cm. The maximum current in an individual strip is about 0.3 A. This leads to a maximum temperature rise on the order of 10 °C, which is insufficient to cause significant changes in the metal-polymer adhesion. However, if we consider the beginning of the plating process just after generation of a very thin layer of catalytic palladium salts, the metal thickness is much lower; moreover, the conductivity of palladium is only about 20% of that for copper. Consequently, an initial temperature rise on the order of 100 °C may occur, which could influence adhesion. This temperature would only be maintained for a short time as the deposit thickness grew, and a temperature that significantly exceeds the boiling point of the solution could not be attained in thin strips. Further studies are needed to elucidate the mechanisms that are responsible for the increase in adhesive strength with increasing current density.

As mentioned above, a plausible mechanism for the increase in adhesion with heating is an increase the state of cure (SOC) at higher temperature in the polyimide layer, especially at the interface with the catalyst layer. Our analysis with Fourier transform infrared spectroscopy (FTIR) to determine SOC (characterized by percent imidization) showed a correlation between SOC and peel strength. As peel strength increased from 1 to 6.5 lb in^{-1}, the SOC increased by about 15% .

We performed a series of experimental analyses, using secondary ion mass spectroscopy, depth profiling, and FTIR, to determine the location and mode of failure in the peel test. We found that adhesive failure was observed at the copper/catalytic layer interface at low values of peel strength. At high values of peel strength, a cohesive failure within the catalyst layer was observed. We also found that elemental oxygen was present on the peeled side of the copper strip on samples with strong adhesion. These results suggest that copper oxide or similar compounds are formed at the interface when good adhesion is achieved.

The transition between these two modes of failure was found to occur at about 2.3 lb in^{-1}. In Fig. 4 we see that a steep drop in peel strength occurs at a distance of about 250 mm along the cathode. The peel strength at that point is near the 2.3 lb in^{-1} transition point, and we can attribute this sharp drop to a change in mechanism from cohesive to adhesive failure.

8. Conclusions

From samples obtained using a modified Hull cell, we determined that the adhesion of copper electrodeposits on a polyimide substrate increased with increasing current density. The detailed mechanisms responsible for the increase in adhesive strength with increasing current density are unknown to us at present, and further studies are needed to elucidate them. Peel tests were performed on a series of strips plated onto a polyimide substrate. Acceptable adhesion values of about 6 lb in^{-1} were obtained at the highest current density, estimated to be about 0.025 A cm^{-2}. Samples below the average current density of 0.01 A cm^{-2} gave unacceptable adhesion values of about 1 lb in^{-1}.

In these experiments the Hull cell was successfully used to produce a range of current densities on a single sample for rapid screening for acceptable ranges. From our simulations we were able to make an estimate of the local current densities. The test procedure developed should be generally applicable to other metal-polymer systems.

Acknowledgements

This work was supported by the United States Department of Energy under contract DE-AC04-94AL85000. Sandia is a multiprogram laboratory operated by Sandia Corporation, a Lockheed Martin Company, for the United States Department of Energy. We wish to acknowledge the assistance of Dr Jianwei Li at University of Detroit Mercy for developing the polarization curves. We would also like to acknowledge Messrs J. Zich, W. Morgan and M. Starig of Sandia National Laboratories for help in preparing metallized samples and for performing peel strength measurements.

References

[1] K. L. Mittal and J. R. Susko, 'Metallized Plastics 1: Fundamental and Applied Aspects', Plenum Press, New York (1989).
[2] B. R. Karas, D. F. Foust and G. M. Porta, *J. Adhesion Sci. Technol.* **6** (1992) 557.
[3] S. Bhansali and D. K. Sood, *Thin Solid Films* **270** (1995) 489.
[4] P. Bindra and J. R. White, Fundamental aspects of electroless copper plating, *in* '*Electroless Plating*' (edited by G. O. Mallory and J. B. Hajdu), American Electroplaters and Surface Finishers Society, FA (1990), p. 289.
[5] F. E. Stone, Electroless copper in printed wiring board fabrication, *in* '*Electroless Plating*' ,*op.cit*. [4], p. 331.
[6] E. F. Tokas, R. M. Shaltout and K. S. Chen, 'Metal Coated Polyimide', *US Patent 5348574* (1994).
[7] C. E. Baumgarnter, *Plati. Surf. Finish.* **79** (1992) 53.
[8] C. E. Baumgarnter and L. R. Scott, *J. Adhesion Sci.* **9** (1995) 789.
[9] L. J. Krause and T. A. Speckhard, An electrochemical method of polyimide metallization, *in* '*Metallized Plastics 2*' (edited by K. L. Mittal), Plenum Press, New York (1991), p. 3.
[10] G. A. Prentice, Numerical techniques for modeling of cells with plane or flow-by electrodes, *in* 'Techniques for Characterization of Electrodes and Electrochemical Processes' (edited by R. Varma and J. R. Selman), J. Wiley & Sons, New York (1991), p. 649.
[11] G. A. Prentice, 'Electrochemical Engineering Principles', Prentice Hall, Englewood Cliffs, NJ (1991), chapter 6.
[12] M. Matlosz, C. Creton, C. Clerc and D. Landolt, *J. Electrochem. Soc.* **134** (1987) 3015.